



ACADEMIC
PRESS

Available online at www.sciencedirect.com

SCIENCE @ DIRECT®

Journal of Sound and Vibration 261 (2003) 573–582

JOURNAL OF
SOUND AND
VIBRATION

www.elsevier.com/locate/jsvi

Letter to the Editor

A closed-form formulation for earthquake-induced hydrodynamic pressure on gravity dams

N. Bouaanani, P. Paultre*, J. Proulx

Department of Civil Engineering, University of Sherbrooke, Sherbrooke, Que., Canada J1K 2R1

Received 21 February 2002; accepted 9 August 2002

1. Introduction

Computing the hydrodynamic pressures exerted on the upstream face of dams is of chief interest in designing and evaluating the safety of these structures in seismically active regions. Since the classical work by Westergaard [1], the question has attracted a considerable amount of research attention. In parallel with various methods proposed by researchers, ranging from finite element modelling to boundary integral equations, some simplified formulations were derived for the need of practicing designers. However, these simplified formulas are generally based on many restricting assumptions, such as neglecting water compressibility and reservoir bottom absorption. Numerical studies carried out with models that account for these energy dissipating mechanisms in the reservoir, have shown that the changes to the hydrodynamic pressure can be considerably important, and moreover not always on the conservative side [2]. This paper presents an easy-to-use technique to get a reliable estimate of the earthquake-induced hydrodynamic pressures on gravity dams, by proposing closed-form formulas for the eigenvalues involved when solving the fluid–dam interaction problem.

2. A review of the theory

The approach presented herein is based on the procedure derived by Fenves and Chopra in Ref. [2]. The basic concepts underlying this formulation are reviewed in this paper, and the same notation as in Ref. [2] is used.

Let us consider a gravity dam with a vertical upstream face, impounding a reservoir of constant depth, H , and extending to infinity in the upstream direction (Fig. 1). The dam and the reservoir are supported on a flexible foundation modeled as a viscoelastic half-plane. The following

*Corresponding author. Tel.: +1-819-921-7114; fax: +1-819-821-7108.

E-mail address: patrick.paultre@courrier.usherb.ca (P. Paultre).

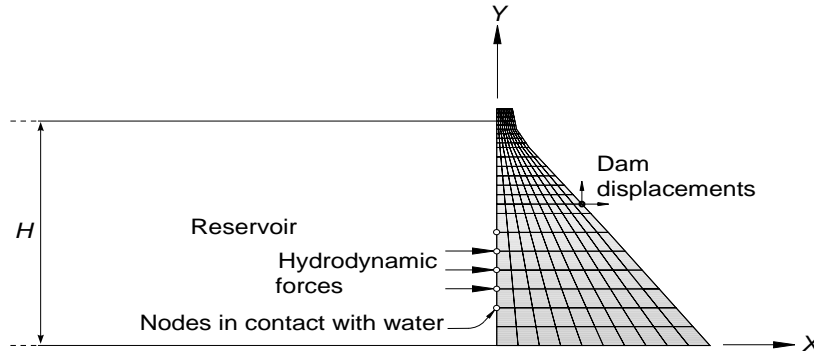


Fig. 1. The dam-reservoir system (adapted from Fenves and Chopra [2]).

assumptions are considered in the formulation of equations:

- The dam, the water and the foundation are assumed to have a linear behavior.
- The dam–reservoir–foundation system is treated as two-dimensional.
- The reservoir is assumed to have regular rectangular boundaries.
- The water in the reservoir is compressible and inviscid, with its motion irrotational and limited to small amplitudes.
- The exciting ground acceleration is assumed to be harmonic and horizontal.
- Gravity surface waves are neglected.

Under these assumptions, the hydrodynamic pressure p in the reservoir (in addition to the hydrostatic pressure) obeys the following equations:

$$\frac{\partial p}{\partial x} = -\rho_w \frac{\partial^2 u}{\partial t^2}, \quad (1)$$

$$\frac{\partial p}{\partial y} = -\rho_w \frac{\partial^2 v}{\partial t^2}, \quad (2)$$

$$\frac{\partial^2 p}{\partial x^2} + \frac{\partial^2 p}{\partial y^2} = \frac{1}{C^2} \frac{\partial^2 p}{\partial t^2}, \quad (3)$$

where x and y are the Cartesian co-ordinates as illustrated in Fig. 1; u and v are the x and y components of the displacement of a water particle, respectively; t is the time variable; ρ_w the mass density of water and C the velocity of sound in water.

For harmonic ground motion, the pressure in the reservoir can be expressed in the frequency domain as $p(x, y, t) = \bar{p}(x, y, \omega)e^{i\omega t}$, where ω is the exciting frequency and $\bar{p}(x, y, \omega)$ the complex-valued frequency response function for hydrodynamic pressure. Using this transformation into Eq. (3) yields the classical Helmholtz equation:

$$\frac{\partial^2 \bar{p}}{\partial x^2} + \frac{\partial^2 \bar{p}}{\partial y^2} + \frac{\omega^2}{C^2} \bar{p} = 0. \quad (4)$$

The boundary conditions to be satisfied by Eq. (4) are as follows:

- (1) The acceleration boundary condition at the interface of the dam and reservoir

$$\frac{\partial \bar{p}}{\partial n}(0, y, \omega) = -\rho_w a_n(0, y, \omega) \tag{5}$$

in which n denotes the inward normal direction to a boundary and $a_n(x, y, \omega)$ the normal component of boundary acceleration.

- (2) The acceleration boundary condition at the reservoir and foundation interface

$$\frac{\partial \bar{p}}{\partial n}(x, 0, \omega) = i\omega q \bar{p}(x, 0, \omega), \tag{6}$$

where q is the damping coefficient of the reservoir bottom defined as

$$q = \frac{\rho_w}{\rho_f C_f} \tag{7}$$

and where ρ_f and C_f are, respectively, the mass density and the compression-wave velocity of the foundation. The portion of the wave amplitude reflected back to the reservoir can then be represented by the wave reflection coefficient α defined by

$$\alpha = \frac{1 - Cq}{1 + Cq} \tag{8}$$

where α may vary from 0, for full wave absorption, to 1, for full wave reflection.

- (3) The zero pressure condition at the free surface is

$$\bar{p}(x, H, \omega) = 0. \tag{9}$$

- (4) And finally, the radiation condition

$$\lim_{x \rightarrow -\infty} \bar{p}(x, y, \omega) = 0. \tag{10}$$

To summarize, the pressure field in the rectangular reservoir is governed by the following boundary conditions:

$$\frac{\partial \bar{p}}{\partial x}(0, y, \omega) = -\rho_w a_n(0, y, \omega), \tag{11}$$

$$\frac{\partial \bar{p}}{\partial y}(x, 0, \omega) = i\omega q \bar{p}(x, 0, \omega), \tag{12}$$

$$\bar{p}(x, H, \omega) = 0, \tag{13}$$

$$\lim_{x \rightarrow -\infty} \bar{p}(x, y, \omega) = 0. \tag{14}$$

When the excitation is caused by a harmonic horizontal acceleration $e^{i\omega t}$, the normal frequency response acceleration of a point $(x = 0, y)$ belonging to the rigid dam face is simply

$$a_n(0, y, \omega) = 1. \tag{15}$$

Using the method of separation of variables, it can be shown that solving Eq. (4) leads to a Sturm–Liouville problem, with complex-valued frequency dependent eigenvalues $\lambda_n(\omega)$ of the impounded water and orthogonal eigenfunctions $Y_n(y, \omega)$ satisfying

$$e^{2i\lambda_n(\omega)H} = -\frac{\lambda_n(\omega) - \omega q}{\lambda_n(\omega) + \omega q} \quad \text{for } n = 1, 2, 3, \dots \quad (16)$$

and

$$Y_n(y, \omega) = \frac{1}{2\lambda_n(\omega)} [(\lambda_n(\omega) + \omega q)e^{i\lambda_n(\omega)y} + (\lambda_n(\omega) - \omega q)e^{-i\lambda_n(\omega)y}]. \quad (17)$$

Eq. (16) is generally solved for each excitation frequency ω in the range of interest by using iterative solutions such as the Newton–Raphson method implemented in the finite element program EAGD [3]. The method requires an initial guess for the roots, the evaluation of both a function and its derivative and converges after a certain number of iterations. Once the eigenvalues are determined, the complex-valued pressure frequency response functions $\bar{p}(x, y, \omega)$ at point x, y of the reservoir can be found as

$$\begin{aligned} \bar{p}(x, y, \omega) &= -2\rho_w H \sum_{n=1}^{\infty} \frac{\lambda_n^2(\omega) I_{0n}(\omega)}{\beta_n(\omega) \kappa_n(\omega)} e^{\kappa_n(\omega)x} Y_n(y, \omega) \\ &\approx -2\rho_w H \sum_{n=1}^N \frac{\lambda_n^2(\omega) I_{0n}(\omega)}{\beta_n(\omega) \kappa_n(\omega)} e^{\kappa_n(\omega)x} Y_n(y, \omega), \end{aligned} \quad (18)$$

where

$$I_{0n}(\omega) = \frac{1}{H} \int_0^H Y_n(y, \omega) dy, \quad (19)$$

$$\beta_n(\omega) = (\lambda_n^2(\omega) - \omega^2 q^2)H + i\omega q, \quad (20)$$

$$\kappa_n(\omega) = \sqrt{\lambda_n^2(\omega) - \frac{\omega^2}{C^2}}, \quad (21)$$

and where N is the number of significant reservoir vibration modes to be included in the analysis [2].

It is clear that a rigorous solution to the problem depends on the determination of the eigenvalues λ_n , which generally requires the use of a specialized software [3] or advanced programming techniques. In this paper, an alternative strategy based on finding approximate expressions for the eigenvalues λ_n is proposed.

3. Approximation of eigenvalues

Introducing $z_n = \lambda_n(\omega)/q$, Eq. (16) becomes

$$e^{2iz_n H q} = -\frac{z_n - \omega}{z_n + \omega} \quad \text{for } n = 1, 2, 3, \dots \quad (22)$$

Performing derivation with respect to ω gives

$$iHq z'_n e^{2iz_n Hq} = \frac{z_n - \omega z'_n}{(z_n + \omega)^2} \quad \text{for } n = 1, 2, 3, \dots \tag{23}$$

in which z'_n denotes the derivative of z_n with respect to ω .

Substitution of the expression for $e^{2iz_n Hq}$ from Eq. (22) into Eq. (23) results in

$$iHq z'_n \frac{\omega - z_n}{z_n + \omega} = \frac{z_n - \omega z'_n}{(z_n + \omega)^2} \quad \text{for } n = 1, 2, 3, \dots \tag{24}$$

which after simplification gives the non-linear differential equation

$$z'_n = \frac{z_n}{\omega + iHq(\omega^2 - z_n^2)} \quad \text{for } n = 1, 2, 3, \dots \tag{25}$$

It can be demonstrated and argued through numerical examples that for large values of the reflection coefficient α , the terms ω and ω^2 are relatively small compared to the other terms in Eq. (25), and they can be dropped without introducing significant error as will be shown later. Hence, we can assume that under some conditions that will be shown when assessing the range of validity of this approximation, Eq. (25) simplifies to

$$z'_n = \frac{i}{Hqz_n} \quad \text{for } n = 1, 2, 3, \dots \tag{26}$$

or, after separation of variables,

$$z_n dz_n = \frac{i}{Hq} d\omega \quad \text{for } n = 1, 2, 3, \dots \tag{27}$$

Finally, integration between 0 and ω of Eq. (27) yields

$$z_n^2(\omega) = z_n^2(0) + \frac{2i\omega}{Hq} \quad \text{for } n = 1, 2, 3, \dots \tag{28}$$

or, getting back to λ_n ,

$$\lambda_n^2(\omega) = \lambda_n^2(0) + i \frac{2\omega q}{H} = \frac{(2n - 1)^2 \pi^2}{(2H)^2} + i \frac{2\omega q}{H} \quad \text{for } n = 1, 2, 3, \dots, \tag{29}$$

where $\lambda_n(0) = (2n - 1)\pi/2H$ are the roots of Eqs. (16) for $\omega = 0$.

Hence the coefficients $\beta_n(\omega)$ and $\kappa_n(\omega)$ can be obtained by using Eq. (29), as

$$\beta_n(\omega) = H \left[\frac{(2n - 1)^2 \pi^2}{(2H)^2} - \omega^2 q^2 \right] + 3i\omega q \tag{30}$$

and

$$\kappa_n^2(\omega) = \left[\frac{(2n - 1)^2 \pi^2}{(2H)^2} - \frac{\omega^2}{C^2} \right] + i \frac{2\omega q}{H}. \tag{31}$$

From expressions (29)–(31) one can also derive recurrence formulas for λ_n , β_n and κ_n as follows:

$$\lambda_{n+1}^2(\omega) = \lambda_n^2(\omega) + 2n\frac{\pi^2}{H^2}, \quad (32)$$

$$\beta_{n+1}(\omega) = \beta_n(\omega) + 2n\frac{\pi^2}{H}, \quad (33)$$

$$\kappa_{n+1}^2(\omega) = \kappa_n^2(\omega) + 2n\frac{\pi^2}{H^2}. \quad (34)$$

Using Eq. (22) and performing integration, the coefficient $I_{0n}(\omega)$ given by Eq. (19) can be expressed as

$$I_{0n}(\omega) = \frac{ie^{-i\lambda_n H}}{\lambda_n H} \left[\frac{\lambda_n}{\lambda_n + \omega q} - \frac{\omega^2 q^2}{\lambda_n(\lambda_n + \omega q)} + \frac{\omega q e^{i\lambda_n H}}{\lambda_n} \right]. \quad (35)$$

Again, it can be justified numerically that the terms $\omega^2 q^2 / \lambda_n(\lambda_n + \omega q)$ and $\omega q e^{i\lambda_n H} / \lambda_n$ can be neglected in the equation without significant loss of accuracy. Eq. (35) simplifies then to

$$I_{0n}(\omega) = \frac{ie^{-i\lambda_n H}}{H(\lambda_n + \omega q)}. \quad (36)$$

4. Pressures at dam face

From this point on, the pressure at dam face ($x = 0$) will be denoted by $\bar{p}(y, \omega)$. According to Eqs. (18) and (17), we can write

$$\begin{aligned} \bar{p}(y, \omega) &= -2\rho_w H \sum_{n=1}^N \frac{\lambda_n^2(\omega)}{\beta_n(\omega)} \frac{I_{0n}(\omega)}{\kappa_n(\omega)} Y_n(y, \omega) \\ &= -2\rho_w H \sum_{n=1}^N S(n, y, \omega), \end{aligned} \quad (37)$$

where $S(n, y, \omega)$ denotes the terms under the summation sign.

Then, the real and imaginary parts of $S(n, y, \omega)$ can be expressed as

$$\begin{aligned} \text{Re}[S(n, y, \omega)] &= -\frac{\sqrt{2}}{4H} \left[\frac{S_{12}\sqrt{S_4 + S_2} - S_{11}\sqrt{S_4 - S_2}}{S_4 S_{13}} (S_6 + \omega q) \right. \\ &\quad \left. - \frac{S_{11}\sqrt{S_4 + S_2} + S_{12}\sqrt{S_4 - S_2}}{S_4 S_{13}} S_5 \right] \end{aligned} \quad (38)$$

and

$$\begin{aligned} \text{Im}[S(n, y, \omega)] = \frac{\sqrt{2}}{4H} & \left[\frac{S_{11}\sqrt{S_4 + S_2} + S_{12}\sqrt{S_4 - S_2}}{S_4 S_{13}}(S_6 + \omega q) \right. \\ & \left. + \frac{S_{12}\sqrt{S_4 + S_2} - S_{11}\sqrt{S_4 - S_2}}{S_4 S_{13}} S_5 \right], \end{aligned} \tag{39}$$

where the S_i coefficients can be derived from Eqs. (29)–(31) and (36) through straightforward but tedious manipulations, yielding

$$\begin{aligned} S_0 &= \frac{(2n - 1)^2 \pi^2}{4H^2}, \quad S_1 = S_0 - \omega^2 q^2, \quad S_2 = 4 \left(S_0 - \frac{\omega^2}{C^2} \right), \\ S_3 &= 4 \sqrt{S_0^2 + 4 \frac{\omega^2 q^2}{H^2}}, \quad S_4 = \sqrt{S_2^2 + 64 \frac{\omega^2 q^2}{H^2}}, \\ S_5 &= \frac{1}{4} \sqrt{2(S_3 - 4S_0)}, \quad S_6 = \frac{1}{4} \sqrt{2(S_3 + 4S_0)}, \\ S_7 &= 2[S_5 \cos(S_6 H) - S_6 \sin(S_6 H)] e^{S_5 H}, \\ S_8 &= 2[S_6 \cos(S_6 H) + S_5 \sin(S_6 H)] e^{S_5 H}, \\ S_9 &= [(S_6 + \omega q) e^{-S_5 y} + (S_6 - \omega q) e^{S_5 y}] \cos(S_6 y) + [e^{S_5 y} - e^{-S_5 y}] S_5 \sin(S_6 y), \\ S_{10} &= [e^{-S_5 y} + e^{S_5 y}] S_5 \cos(S_6 y) + [(S_6 + \omega q) e^{-S_5 y} - (S_6 - \omega q) e^{S_5 y}] \sin(S_6 y), \\ S_{11} &= \frac{(S_8 S_9 - S_7 S_{10}) S_1 H}{A_1^2 H^2 + 9 \omega^2 q^2} + 3 \frac{(S_7 S_9 + S_8 S_{10}) \omega q}{A_1^2 H^2 + 9 \omega^2 q^2}, \\ S_{12} &= \frac{(S_7 S_9 + S_8 S_{10}) S_1 H}{A_1^2 H^2 + 9 \omega^2 q^2} - 3 \frac{(S_8 S_9 - S_7 S_{10}) \omega q}{A_1^2 H^2 + 9 \omega^2 q^2}, \\ S_{13} &= -\frac{S_0}{2} + \frac{S_3}{8} + (S_6 + \omega q)^2. \end{aligned}$$

Summing up the contributions of each impounded water mode, the total pressure at co-ordinate y at dam face can be finally expressed as

$$\bar{p}(y, \omega) = -2\rho_w H \left[\sum_{n=1}^N \text{Re}[S(n, y, \omega)] + i \sum_{n=1}^N \text{Im}[S(n, y, \omega)] \right]. \tag{40}$$

5. Illustrative example

To assess the effectiveness and the range of applicability of the proposed computational method, the 84-m Outardes 3 gravity dam reservoir is considered for analysis in this section. The dam was subject to extensive dynamic large-scale tests by the Earthquake Engineering and Structural Dynamics Research Center of the University of Sherbrooke (CRGP) under summer and harsh winter conditions [4]. The reservoir is assumed to have a rectangular geometry as shown

in Fig. 1, with a height of $H = 70$ m and a far end at $L = 2H = 140$ m. In this example, the water is assumed compressible, with the following properties : velocity of pressure waves $C = 1440$ m/s, and a mass density $\rho = 1000$ kg/m³. The hydrodynamic pressure exerted on the dam face was determined using the simplified formulation proposed in the previous section and the classical numerical solution developed in Ref. [3]. The pressures were determined for different values of the frequency ratio $\omega/\bar{\omega}$, where $\bar{\omega} = \pi C/(2H)$ is the natural frequency of the reservoir.

By observing the approximations leading to Eqs. (26) and (36), one can see that the accuracy of the proposed simplified formulation depends essentially on the wave reflection coefficient α representing the reservoir bottom absorption. To have a good understanding of the effect of this parameter, several situations were studied where the wave reflection coefficient is varied over a wide range. Results are presented in this paper for five different values of α , 0.25, 0.50, 0.75, 0.925. Note that values of α in the range 0.5–1 are most frequent, and that the value of 0.925 was selected from the numerical correlation studies carried out with the on-site dynamic investigation at Outardes 3 dam [4].

6. Results

Figs. 2a–d show the variations of hydrodynamic pressure along the dam face at reservoir resonance ($\omega/\bar{\omega} = 1$) and for different values of the wave reflection coefficient α . As can be

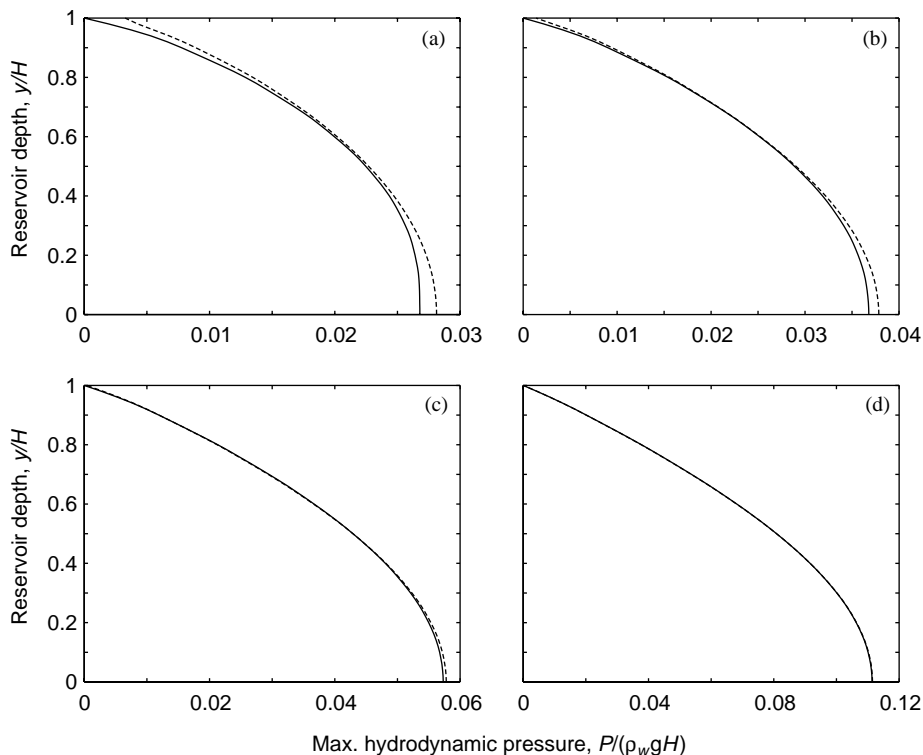


Fig. 2. Hydrodynamic pressure distribution on dam face. - - -, present method; — classical solution. (a) $\alpha = 0.25$, (b) $\alpha = 0.50$, (c) $\alpha = 0.75$, and (d) $\alpha = 0.925$.

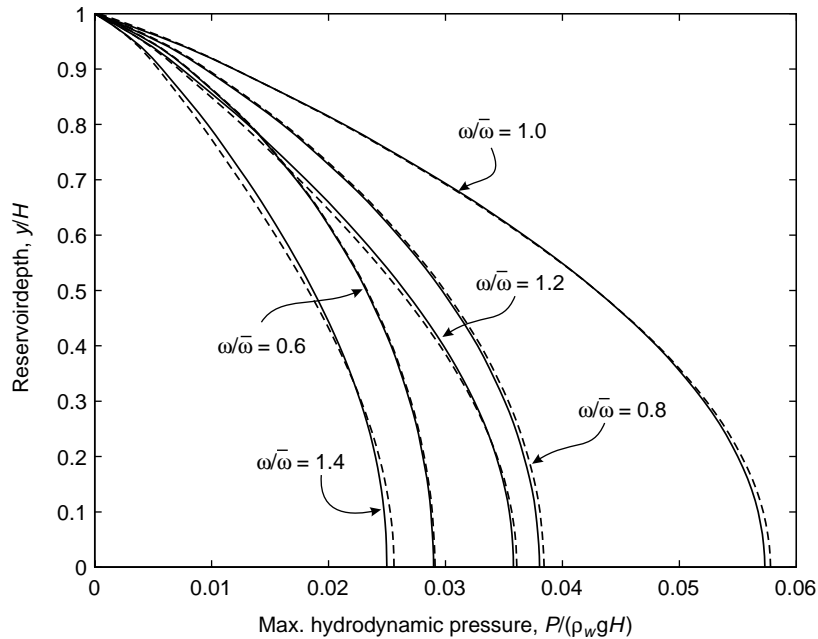


Fig. 3. Hydrodynamic pressure distribution for different frequency ratios $\omega/\bar{\omega}$ and for $\alpha = 0.75$: - - -, present method; — classical solution.

observed, the agreement of the simplified solution proposed herein with the classical formulation is excellent for reservoirs with high values of the reflection coefficients. Results for those with lower values of α also show good agreement with a slight increase in pressure. However, Figs. 2(a) and (b) reveal that the hydrodynamic pressure at water surface is not equal to zero due to the simplifications adopted in the formulation.

To illustrate the influence of the frequency ratio $\omega/\bar{\omega}$ on the accuracy of the proposed method, Fig. 3 portrays pressure distributions obtained for different frequency ratios and with a moderate value of the reflection coefficient ($\alpha = 0.75$). Again, the curves clearly show an excellent agreement for this type of reservoir bottom absorption condition, and even better correlations are obtained when $\alpha > 0.75$. The same correlation can be observed in Fig. 4, which presents a plot of the frequency response curves of the maximum pressure at the dam heel obtained using both methods over a frequency range from 0 to 20 Hz.

7. Conclusions

The paper has presented a new approximate analytical technique for earthquake-induced hydrodynamic pressures on rigid gravity dams allowing for water compressibility and wave absorption at the reservoir bottom. The results obtained are in good agreement with other classical solutions. In addition to the fact that the method can be easily incorporated in a dam structural analysis program by using a set of formulas instead of solving the eigenvalue problem

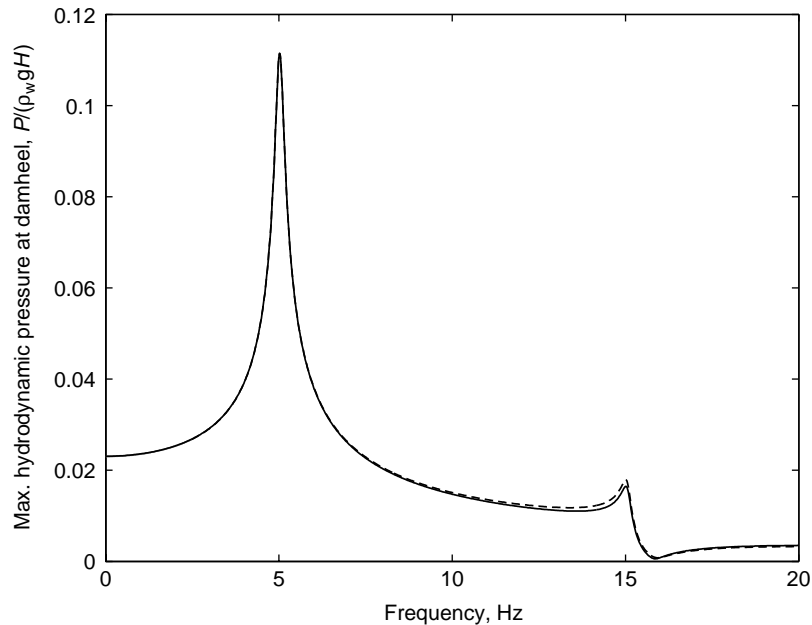


Fig. 4. Frequency response curves for hydrodynamic pressure at upstream dam heel for $\alpha = 0.925$. - - -, present method; — classical solution.

through a numerical technique, the procedure proposed transforms the eigenvalue problem to a differential equation, thus providing an alternative approach to finding the eigenvalues. Also, other benefits of this method is that it can be extended to situations where the reservoir is subjected to other boundary conditions, such as the presence of an ice cover or gravity waves.

Acknowledgements

The authors acknowledge the financial support of the Natural Sciences and Engineering Research Council of Canada and Hydro-Quebec. The authors are also grateful to Mr. Tai Mai Phat of Hydro-Quebec for his continued collaboration.

References

- [1] H.M. Westergaard, Water pressures on dams during earthquakes, Transactions of the American Society of Civil Engineers 98 (1933) 418–433.
- [2] G. Fenves, A.K. Chopra, Earthquake analysis and response of concrete gravity dams, Report No UCB/EERC-84/10, 1984.
- [3] G. Fenves, A.K. Chopra, A computer program for earthquake analysis of concrete gravity dams. Report No UCB/EERC-84/11, EAGD-84, 1984.
- [4] J. Proulx, P. Paultre, Experimental and numerical investigation of dam–reservoir–foundation interaction for a large gravity dam, Canadian Journal of Civil Engineering 24 (1) (1997) 90–105.